

Progress Report
AFOSR Contract F49620-02-1-0176
Jerrold E. Marsden (Caltech) and
Kamran Mohseni (University of Colorado)
July, 2005

Progress has been made on the following topics.

1. Averaged fluid equations: the LANS- α and CLANS- α equations
2. Simulations of the compressible CLANS- α equations
3. Dynamic α formulation and computations for turbulent flow
4. The Helmholtz deconvolution model
5. Optimal control in a dynamic environment
6. The EPDiff Equations
7. Flow simulation around a Micro Air Vehicle (MAV)

1 Averaged Fluid Equations: the LANS- α and CLANS- α Equations

We have derived, in a mathematically precise way, Lagrangian averaged models for incompressible and compressible flow. This work has now appeared in the SIAM journal *Multiscale Modeling and Simulation*; Bhat, Fetecau, Marsden, Mohseni, and West [2005]. That work lays important foundations for our computational work on the averaged equations as a computational tool for shocks.

The **LAE- α equations**: (due to Holm, Marsden and Ratiu in 1998) are

$$\frac{\partial}{\partial t}m + (u \cdot \nabla)m - \alpha^2(\nabla u)^T \cdot \Delta u = -\text{grad } p,$$

where $\alpha > 0$ is a small parameter indicating the subgrid scale, $m = (1 - \alpha^2\Delta)u$, $\text{div } u = 0$, and p is the fluid pressure.

The (much simplified) idea of the derivation of EPDiff and LAE- α is as follows:

1. average *Hamilton's principle* of ideal fluid mechanics over trial curves forming a tube of size α .
2. Expand in terms of α and truncate at α^2
3. Make a *fluctuation advection hypothesis*—a *Taylor hypothesis* (the fluctuations are Lie advected by the main flow)

REPORT DOCUMENTATION PAGE

AFRL-SR-AR-TR-05-

0321

Public reporting burden for this collection of information is estimated to average 1 hour per response, including the time for reviewing instructions, searching existing data sources, gathering and maintaining the data needed, completing and reviewing the collection of information. Send comments regarding this burden estimate or any other aspect of this collection of information, including suggestions for reducing this burden, to Washington Headquarters Services, Directorate for Information Operations and Reports, 1215 Jefferson Davis Highway, Suite 1204, Arlington, VA 22202-4302, and to the Office of Management and Budget, Paperwork Reduction Project (0704-0100), Washington, DC 20503.

1. AGENCY USE ONLY (Leave blank)		2. REPORT DATE	3. REPORT TYPE AND DATES COVERED FINAL REPORT	
4. TITLE AND SUBTITLE COMPRESSIBLE FLOW MODELING WITH THE LAGRANGIAN AVERAGED NAVIER-STOKES-EQUATIONS			5. FUNDING NUMBERS F49620-02-1-0176	
6. AUTHOR(S) PROFESSOR PAUL E. DIMOTAKIS				
7. PERFORMING ORGANIZATION NAME(S) AND ADDRESS(ES) Air Force Office of Scientific Research 875 North Randolph Street Suite 325, Room 3112 Arlington, VA 22203			8. PERFORMING ORGANIZATION REPORT NUMBER	
9. SPONSORING/MONITORING AGENCY NAME(S) AND ADDRESS(ES) CALIFORNIA INSTITUTE OF TECH 1201 E CALIFORNIA BLVD MAIL CODE 202-6 PASADENA, CA 91125			10. SPONSORING/MONITORING AGENCY REPORT NUMBER	
11. SUPPLEMENTARY NOTES				
12a. DISTRIBUTION AVAILABILITY STATEMENT DISTRIBUTION STATEMENT A Approved for Public Release Distribution Unlimited			12b. DISTRIBUTION CODE	
13. ABSTRACT (Maximum 200 words) We have derived, in a mathematically precise way, Lagrangian averaged models for incompressible and compressible flow. This work has now appeared in the SIAM journal Multiscale Modeling and Simulation; Bhat, Fetecau, Marsden, Mohseni, and West [2005]. That work lays important foundations for our computational work on the averaged equations as a computational tool for shocks.				
14. SUBJECT TERMS			15. NUMBER OF PAGES	
			16. PRICE CODE	
17. SECURITY CLASSIFICATION OF REPORT	18. SECURITY CLASSIFICATION OF THIS PAGE	19. SECURITY CLASSIFICATION OF ABSTRACT	20. LIMITATION OF ABSTRACT	

8-2-05

4. This leads to the action function

$$S^\alpha = \int_M \left\{ \frac{1}{2} \|u\|^2 + \frac{\alpha^2}{2} \|\nabla u\|^2 \right\} d^3x.$$

5. (Compute the Euler-Poincaré equations for this averaged action) \Rightarrow LAE- α equations.

While this basic idea for the derivation has been around for some time, the technical details considerably improves earlier ones, even in the incompressible isotropic case and, moreover, it allowed us to make progress on the compressible case as well (see Bhat, Fetecau, Marsden, Mohseni, and West [2005]). A simplified version of what we are doing can be seen from the filtered Lagrangian for 1d compressible flow

$$l(\rho, u) = \int \left(\frac{1}{2} uv - W(\rho) \right) \rho d^N x, \quad (1.1)$$

where $v = (1 - \alpha^2 \partial_{xx})u$.

Obtain the equations of motion from this filtered Lagrangian again the version of Euler-Poincaré theory that contains provision for advected quantities, in this case the density.

Sample calculation shown in Figure 1.1 on equations of this sort show that α controls the width of the shock, independent of the magnitude of (numerical) hyperviscosity that is used and it picks up the correct entropy solution. As in the incompressible turbulent calculations, this should help with resolution issues.

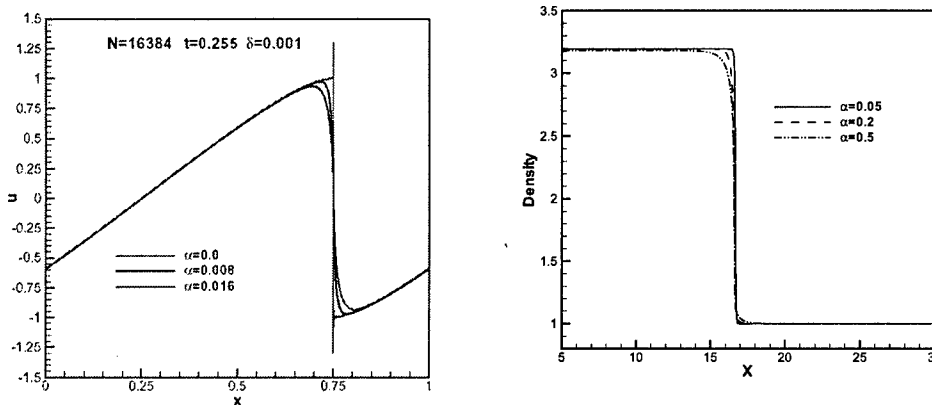


Figure 1.1: Shock regularization by Lagrangian averaging approach. Left: Burgers shock regularization. Right: Normal shock regularization.

2 Dynamic LANS- α Model

In the last workshop and progress report, we reported on progress in turbulent flow calculations for the incompressible case in which averaged isotropic fluid equations accurately

compute the flow at scales above α (see Mohseni, Kosovic, Shkoller and Marsden [2003]), but does not have to resolve scales below α . “The advantages of LES-type models, but there are well-defined pde’s that keep the structure of fluid mechanics.”

We developed a *dynamic* procedure for the Lagrangian Averaged Navier-Stokes- α (LANS- α) equations where the variation in the parameter α in the direction of anisotropy is determined in a self-consistent way from data contained in the simulation itself (see Zhao, Mohseni and Marsden [2004]; Zhao and Mohseni [2004]; Mohseni and Zhao [2005]). The development of the dynamic LANS- α model of this section is a substantial progress in application of the LANS- α model to anisotropic flows, such flow around an airplane. In order to derive this model, the incompressible Navier-Stokes equations are Helmholtz-filtered at the grid and a test filter levels. A Germano type identity is derived as follows by comparing the filtered subgrid scale stress terms with those given in the LANS- α equations.

$$L_{ij} = T_{ij} - \widehat{\tau}_{ij} = \overline{\widehat{u}_i \widehat{u}_j} - \widehat{\overline{u}_i \overline{u}_j}$$

Where $\overline{(\cdot)}$ stands for grid filter and $\widehat{(\cdot)}$ stands for test filter.

Assuming constant α in homogenous directions of the flow and averaging in these directions, results in a nonlinear equation for the parameter α

$$\alpha^2 = F(\alpha) = \frac{\langle L_{ij}(\beta^2 \widehat{N}_{ij} - \widehat{M}_{ij}) \rangle}{\langle (\beta^2 \widehat{N}_{ij} - \widehat{M}_{ij})(\beta^2 \widehat{N}_{ij} - \widehat{M}_{ij}) \rangle}$$

where β is the aspect ratio of test and grid filter width and

$$M_{ij} = \frac{\partial \overline{u}_i}{\partial x_k} \frac{\partial \overline{u}_j}{\partial x_k} - \frac{\partial \overline{u}_k}{\partial x_i} \frac{\partial \overline{u}_k}{\partial x_j} + \frac{\partial \overline{u}_i}{\partial x_k} \frac{\partial \overline{u}_k}{\partial x_j}$$

$$N_{ij} = \frac{\partial \widehat{u}_i}{\partial x_k} \frac{\partial \widehat{u}_j}{\partial x_k} - \frac{\partial \widehat{u}_k}{\partial x_i} \frac{\partial \widehat{u}_k}{\partial x_j} + \frac{\partial \widehat{u}_i}{\partial x_k} \frac{\partial \widehat{u}_k}{\partial x_j}$$

Using the above equations, the parameter α is calculated during the simulation instead of a pre-defined value. Our dynamic model is initially tested in forced and decaying isotropic turbulent flows where α is constant in space but it is allowed to vary in time. It is observed that by using the dynamic LANS- α procedure a more accurate simulation of the isotropic homogeneous turbulence is achieved. The energy spectra and the total kinetic energy decay are captured more accurately as compared with the LANS- α simulations using a fixed α (see Figure 2.1).

In order to evaluate the applicability of the dynamic LANS- α model in anisotropic turbulence, *a priori* test of a turbulent channel flow is performed (see Figure 2.2). It is found that the parameter α changes in the wall normal direction. Near a solid wall, the length scale α is seen to depend on the distance from the wall with a vanishing value at the wall. On the other hand, away from the wall, where the turbulence is more isotropic, α approaches an almost constant value. Furthermore, the behavior of the subgrid scale stresses in the near wall

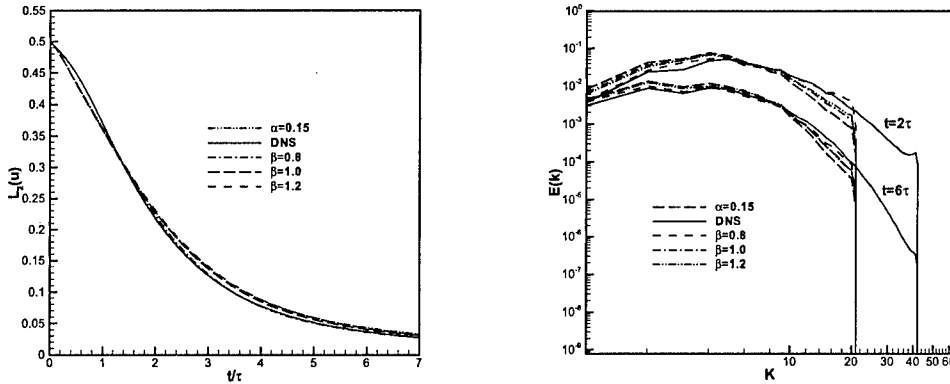


Figure 2.1: Dynamic LANS- α simulation for isotropic homogeneous turbulence. Left: Total kinetic energy decay. Right: Energy spectra snapshots.

region is captured accurately by the dynamic LANS- α model. The dynamic LANS- α model has the potential to extend the applicability of the LANS- α equations to more complicated anisotropic flows.

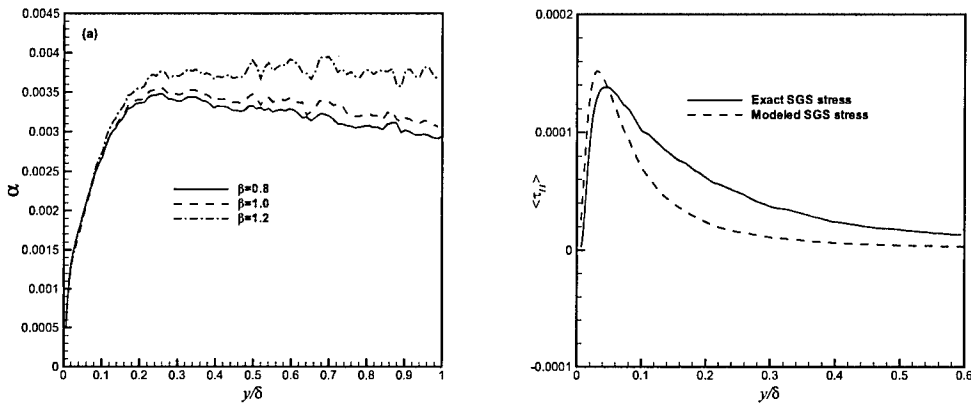


Figure 2.2: A-priori test of dynamic LANS- α model for turbulent channel flow. Left: Variations of α in wall normal direction. Right: Sub-grid stress distribution in wall normal direction.

3 Simulations of the Compressible LANS- α Equations

Numerical Solution and Validation of CLANS- α : In order to test and validate the performance of the CLANS- α equations, one first needs to prepare a database for direct numerical simulation of compressible isotropic turbulence and shock turbulence interaction

using the Navier-Stokes equations. A parallel three-dimensional code, capable of simulating compressible isotropic turbulence and shock-turbulence interaction was developed using a combination of WENO (Weighted Essentially Non-Oscillating) and compact scheme. This scheme has fifth order accuracy in space and it employs a third order Runge-Kutta scheme for time integration. WENO scheme is an efficient technique in shock capturing problems and is particularly effective in simulating shock-turbulence interaction. We have tested and validated our DNS solver by comparing the results with the ones obtained by Pullin, Samtaney and Kosovic [2001]. Figures 3.1 show the comparisons of the total kinetic energy decay and time evolution of the energy spectra in a decaying turbulence case.

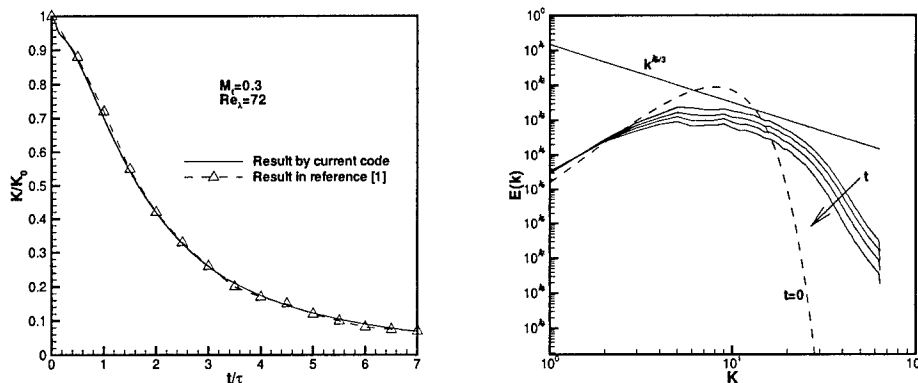


Figure 3.1: Direct numerical simulation of compressible turbulence. Left: Total kinetic energy decay. Right: Energy spectra snapshots and comparison with $k \sim -5/3$ law.

1-D Inviscid Shock Regularization and Shock-Turbulence Interaction Simulation Using the Averaged Euler Equations: A preliminary study of inviscid shock regularization by averaging the convective velocity in Euler equations was performed on a 1-D shock tube problem. It is observed that the shock in pressure are nicely regularized (see Figure 3.2) by replacing the convective term with a Helmholtz filtered velocity $\bar{u} = (1 - \alpha^2 \Delta)^{-1} u$. In this inviscid shock regularization, the shock thickness is controlled by averaging length scale α . We also studied one-dimensional shock-turbulence interaction by this averaged Euler equations. It is found that pressure fluctuation after the shock can be smoothed by increasing the α value in the averaged Euler equation. (see Figure 3.2)

Large Eddy Simulation of Compressible Navier-Stokes Equations: Based on our DNS code, we also developed a code for large eddy simulation of compressible turbulence to be used for testing the accuracy and computational cost of our 3-D CLANS- α model. This code will be used to evaluate the performance of our CLANS- α solver. We have implemented

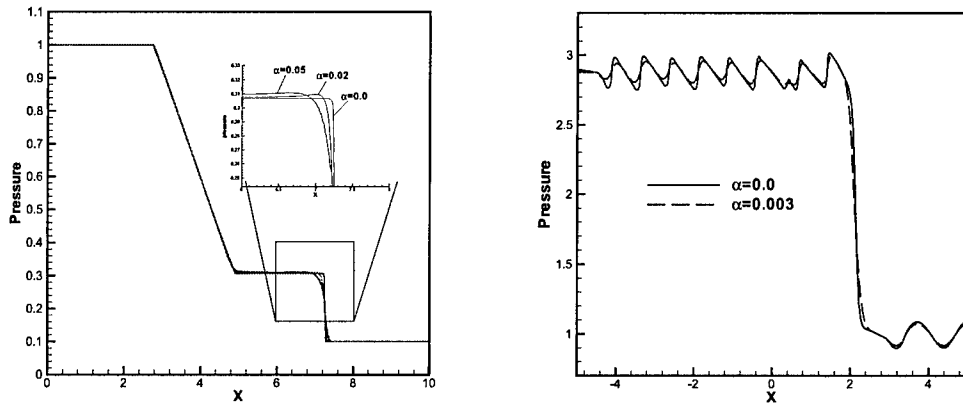


Figure 3.2: Shock regularization and shock-turbulence interaction. Left: Pressure distribution in a shock tube. Right: One-dimensional shock-turbulence interaction.

a Smagorinsky and dynamic Smagorinsky model for sub-grid scale modeling. Figure 3.3 and Figure 3.4 show the LES and dynamic LES simulation results as well as the comparisons with DNS results for isotropic homogenous turbulence.

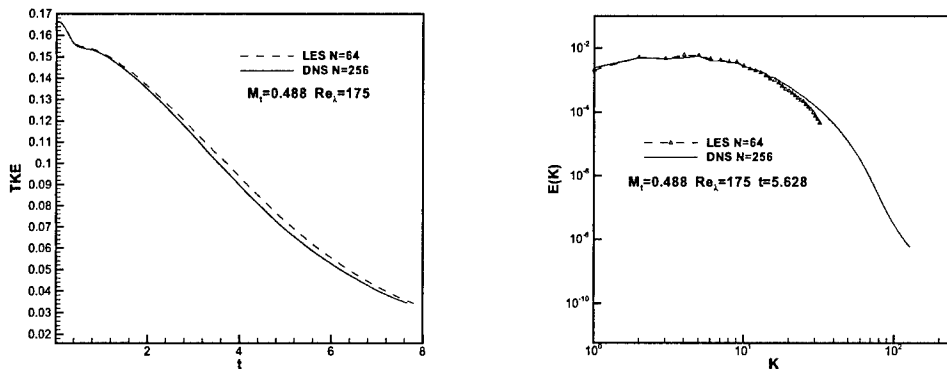


Figure 3.3: Large-eddy simulation of compressible turbulence. Left: Total kinetic energy decay. Right: Energy spectra snapshots.

4 Helmholtz Deconvolution Model

We have already shown that the LANS- α model can accurately capture turbulence scales larger than the scale α Mohseni, Kosovic, Shkoller and Marsden [2003]. Since the Helmholtz

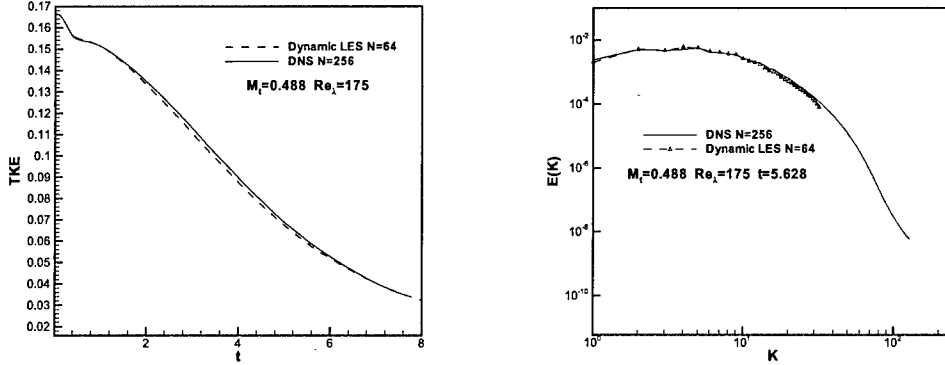


Figure 3.4: Large-eddy simulation of compressible turbulence. Left: Total kinetic energy decay. Right: Energy spectra snapshots.

filter is invertable, the turbulence scales below α may be recovered by a deconvolution operation. This leads us to derive a deconvolution model with Helmholtz filter.

This idea was initiated by A. Jameson (Stanford University) based on our Lagrangian averaging technique. A collaboration with Jameson started in the last AFOSR PI meeting in Dayton Ohio. Following the meeting, we developed a Helmholtz deconvolution model (see Zhao, Mohseni and Jameson [2004]). By substituting Helmholtz decomposed terms $u_i = (1 - \alpha^2 \Delta) \bar{u}_i$ into the incompressible Navier-Stokes equations and rearranging the equations, we can write

$$\rho \frac{\partial \bar{u}_i}{\partial t} + \rho \frac{\partial \bar{u}_i \bar{u}_j}{\partial x_j} = - \frac{\partial \bar{p}}{\partial x_i} + \mu \frac{\partial^2 \bar{u}_i}{\partial x_j \partial x_j} - \rho \frac{\partial \tau_{ij}}{\partial x_j}$$

where

$$\tau_{ij} = \alpha^2 (1 - \alpha^2 \Delta)^{-1} \left[2 \frac{\partial \bar{u}_i}{\partial x_k} \frac{\partial \bar{u}_j}{\partial x_k} + \alpha^2 \frac{\partial^2 \bar{u}_i}{\partial x_k \partial x_k} \frac{\partial^2 \bar{u}_j}{\partial x_l \partial x_l} \right]$$

In order to avoid inverting the Helmholtz operator, one can expand the operator as

$$(1 - \alpha^2 \Delta)^{-1} = 1 + \alpha^2 \Delta + \alpha^4 \Delta^2 + \dots$$

By retaining terms up to the fourth power of α , the approximate virtual stress tensor assumes the following form

$$\tau_{ij} = 2\alpha^2 \frac{\partial \bar{u}_i}{\partial x_k} \frac{\partial \bar{u}_j}{\partial x_k} + \alpha^4 \left[2\Delta \left(\frac{\partial \bar{u}_i}{\partial x_k} \frac{\partial \bar{u}_j}{\partial x_k} \right) + \Delta \bar{u}_i \Delta \bar{u}_j \right]$$

We performed some numerical simulations with this model for isotropic homogenous turbulence. Figure 4.1 shows our preliminary results with spectral vanishing viscosity (SVV). Our Helmholtz deconvolution model provides an accurate sub-grid scale stress model for the decaying isotropic homogenous turbulence simulation in this study. We are in the process of applying this model to more sever test case.

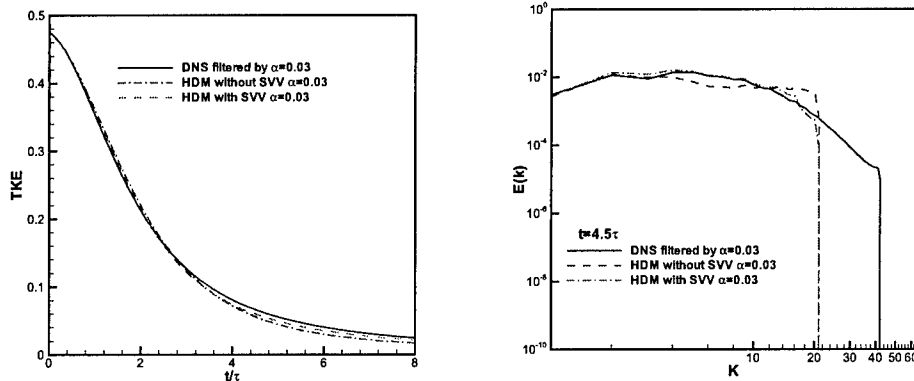
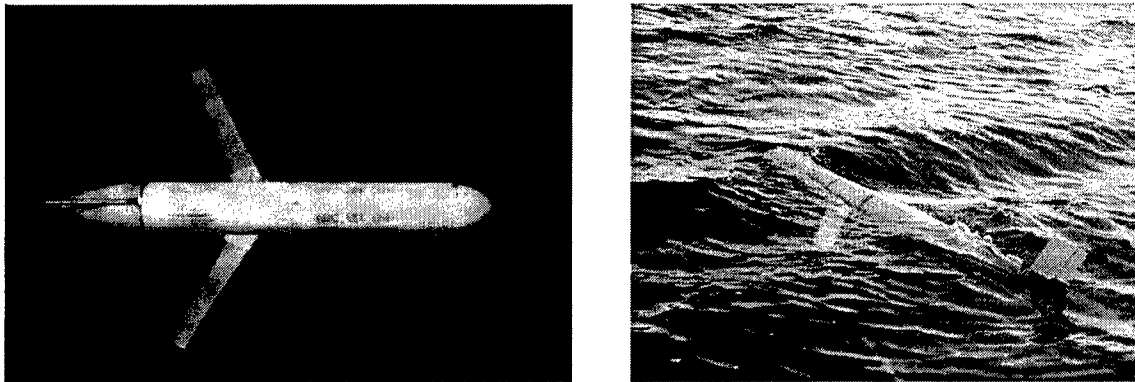


Figure 4.1: Helmholtz deconvolution model in Zhao, Mohseni and Jameson [2004] for isotropic homogenous turbulence simulation. Left: Total kinetic energy decay. Right: Energy spectra snapshots.

5 Optimal Control in a Dynamic Environment

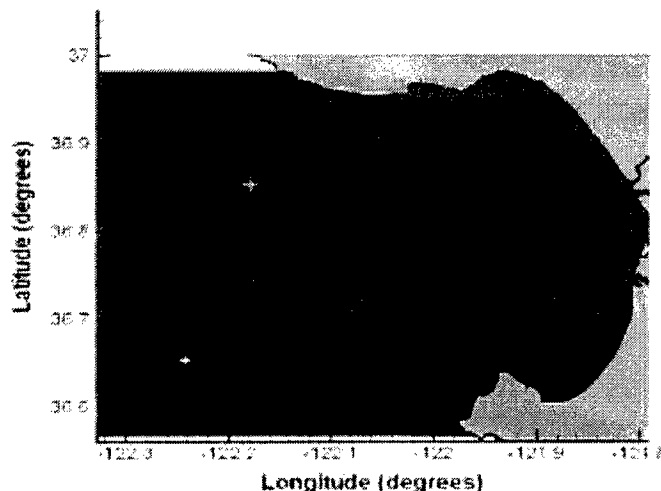
The objective of this project is to do an optimization of underwater gliders in a time dependent ocean environment. This study was motivated by the AOSN-II project (Autonomous Ocean Sampling Network). The results are given in Inanc, Shadden, and Marsden [2005].

The problem involves the control of a simplified model of an underwater glider in Monterey Bay moving in ocean currents whose velocities can be comparable to that of the glider itself.



The objective is to get from point A (the top “cross” in the figure below) to point B (the bottom “cross”), satisfying model equations of motion, and at the same time, optimizing a cost function. In this case, the cost function was a weighted sum of a temporal cost and an energy cost. We then compare the resulting path with Lagrangian coherent structures (LCS), which are regions of expanding (or attracting) material lines and play the role, in the time dependent context, of stable and unstable manifolds. We wanted to test a conjecture, motivated by the use of natural dynamics in other areas, that optimal trajectories are in fact, linked to the use of LCS pathways in the ocean. In this study, this conjecture was verified.

The technique involves several key steps. First of all, we gather data using the Harvard HOPS model for data assimilated from Monterey Bay last summer in August, 2003. We use this data and the software MANGEN (Manifold Generation—Lekien and Couliette) to compute Lagrangian coherent structures for the velocity field so collected. With the same velocity field, we also use the software NTG (Nonlinear Trajectory Generation) to compute the optimal trajectory. Finally, we compare these two independent calculations and see if there is agreement. Indeed, the agreement is remarkably good, indicating that one can use the LCS pathways for optimal planning purposes.



Shane Ross also helped us transition some of the Mangen capabilities from the fluid context to that of transport and mixing in solar system dynamics.

6 The EPDiff Equations

The work described in this section is given in Holm and Marsden [2004]. The n -dimensional *EPDiff equations* are as follows

$$\frac{\partial}{\partial t} m + \underbrace{u \cdot \nabla m}_{\text{convection}} + \underbrace{\nabla u^T \cdot m}_{\text{stretching}} + \underbrace{m(\text{div } u)}_{\text{expansion}} = 0, \text{ the}$$

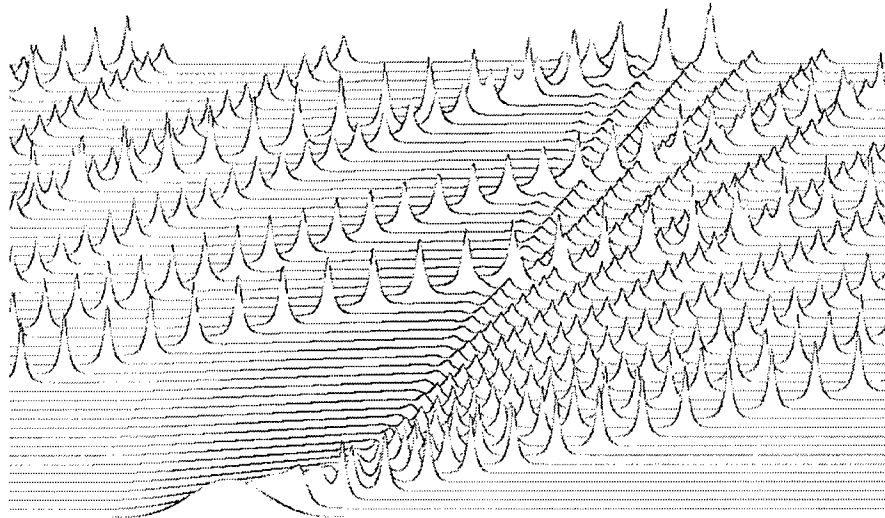
where $m = (1 - \alpha^2 \Delta)u$.

These equations fit into the general theme of averaged equations in fluid mechanics (Euler-Poincaré equations; eg, variational, Hamiltonian structure, Kelvin theorem, etc.). In fact, for $n = 2$, they serve as a model for 2-dimensional waves

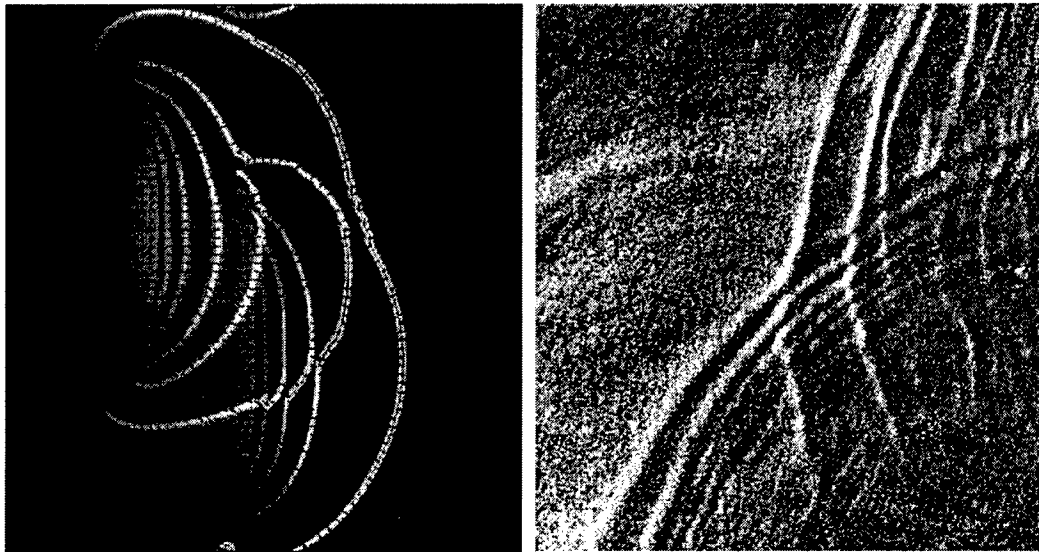
These equations have interesting special *interface solutions*—one of our main contributions is to reveal the rich geometric structure about singular solutions by showing that the solution Ansatz is given by a momentum map relation.

The computation of solutions were done by Martin Staley at Los Alamos—and makes use of mimetic differencing methods; this approach is important to get good resolution of the structures and is related to our idea to eventually implement variational integrators in fluid problems.

The equations in the 1-d case are the Camassa-Holm equations for shallow water waves and the solutions are, as is well-known, dominated by peakons, as in the figure.



The 2-d case, on the other hand, is related to two dimensional waves. The figure shows interface solutions of EPDiff compared to synthetic aperture radar observations (from the Space Shuttle) of internal waves in the South China Sea. It is clear that these special interface solutions of the EPDiff equation are important.



(a)

(b)

In summary, what we did was:

1. Put the problem into the Euler-Poincaré framework (geometric fluid mechanics)
2. Discover the geometry of the interface solutions (eg, that they also evolve by a mechanical structure, have their own conservation laws, etc).

7 Flow Simulation around a Micro Air Vehicle (MAV)

A long term goal of our group is to implement the LANS- α model in simulating turbulent flows in complex geometry. The dynamic LANS- α model reported in section 2 is moving us in that direction. The dynamic LANS- α model allows us to extend the LANS- α calculations to anisotropic flows e.g., close to a wall. We have started to develop our computational capability for simulating flows in complex geometry. This section summarize this effort (also see Mohseni et al [2004]).

A micro air vehicle (MAV) with fixed flexible wings was recently designed, built, and tested in Mohseni's group (see Figure 7.1). The MAV is designed to serve as a platform for characterizing the flight performance of different low Reynolds number wing designs by measuring the in-flight accelerations due to control inputs and gusts. The platform houses an onboard flight computer and communications system that can process sensor information, transmit data to a ground station, and control the aircraft via pilot input from the ground station. With light weight and small wing aspect ratio, the Colorado MAV is susceptible to atmospheric turbulence and gust wind conditions. For optimal design of such a vehicle it is necessary to calculate the aerodynamic characteristic of the MAV.

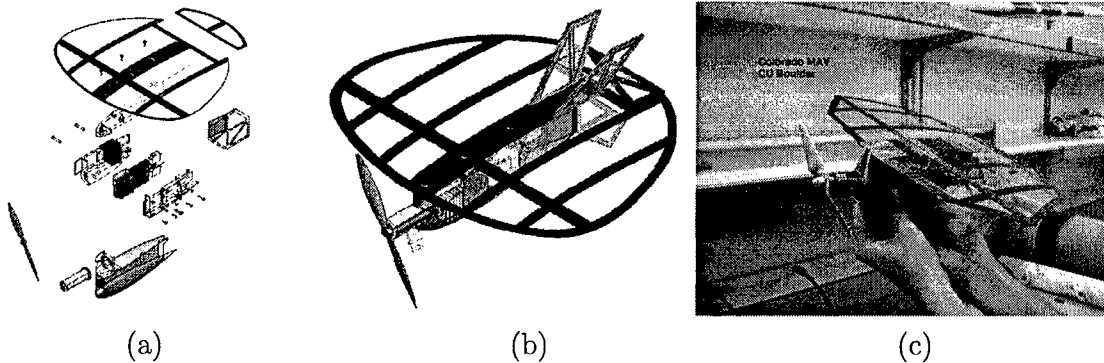


Figure 7.1: Colorado MAV, a flexible wing micro air vehicle designed, fabricated, and tested at the University of Colorado. (a) CAD model assembly, (b) CAD model, (c) CMAV prototype.

A domain decomposition based parallel three-dimensional compressible Euler and Navier-Stokes CFD solver is developed which combines finite volume and finite element discretizations on unstructured tetrahedral meshes. It features an upwind scheme using a piecewise linear reconstruction of the flow variables in each control volume for the convective term, and a P1 finite element Galerkin approximation for the diffusive term.

Starting from the CAD model shown in Figure 7.1(b), an anisotropic grid was generated with 459,000 points and 2.1 million tetrahedra. About 10 layers of stretched elements are located close to the MAV in order to capture accurately the boundary layers. The average thickness of these stretched elements is equal to 10 mm. Figure 7.2 displays several views of the surface mesh as well as a cut along the symmetry plane of the MAV. The refinement on the leading and trailing edges of the wing as well as on the engine can be observed in these figures.

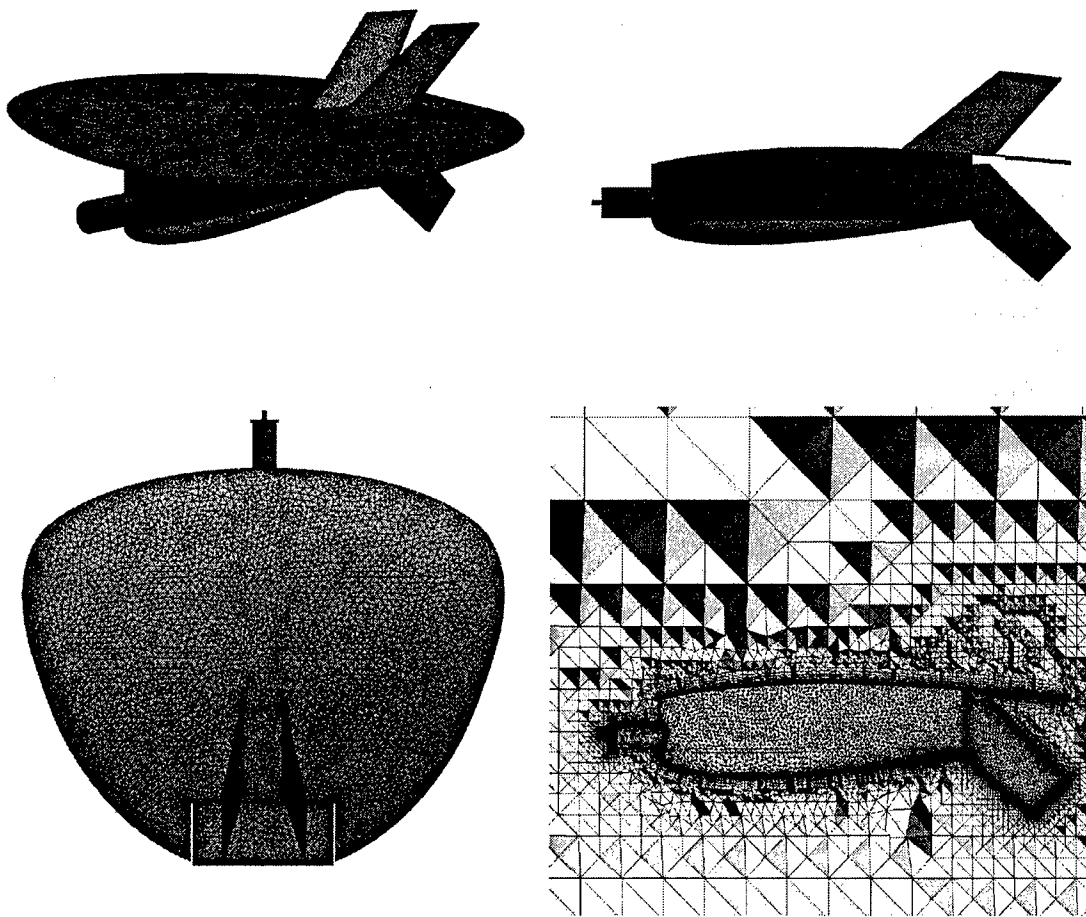


Figure 7.2: Computational grid around the CMAV from Mohseni et al [2004].

The flow is assumed to be viscous and the freestream velocity and the angle of attack are first set respectively to 14 m/s and 15 deg. Figure 7.3 shows the streamlines obtained for these conditions. The freestream velocity and the angle of attack are then varied. Figure 7.4 shows the aerodynamic efficiency curve, where a maximum glide ratio of 3.8 is observed. Similar glide ratio was measured by Waszak and Jenkins [2001] for a flexible wing MAV.

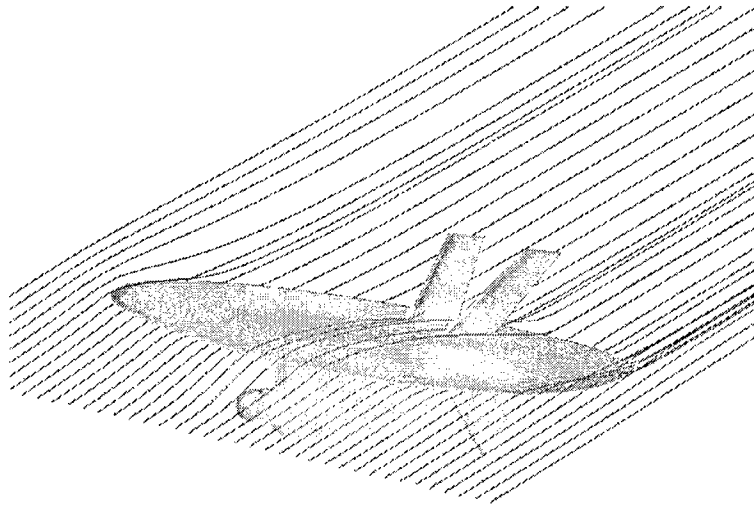


Figure 7.3: Streamlines around the CMAV at 15° AoA. From Mohseni et al [2004]

Increase in flight Reynolds number would increase the lift to drag ratio.

Since the dynamic LANS- α model of section 2 preserve the geometrical structure of the governing equations (e.g, Kelvin circulation) we expect that this model will perform much better in turbulence simulation around MAVs. We are now in the process of implementing a dynamic LANS- α model for the turbulence simulation around the Colorado MAV. This step will move us closer to practical application of the LANS- α modeling in problems of interest in Aerospace industry.

Personell Supported.

Dr. Hongwu Zhao was hired as a reseach associate on July 1, 2003. In the last one year, Dr. Zhao was involved in building the computational capability of testing and validating the ideas in the Lagrangian averaging techniques. In Marsden's group, partial support was given to the graduate students Shane Ross, Razvan Fetecau, Harish Bhat and to the postdoc Tamer Innac who all contributed to this project.

References

Bhat, H. S., R. C. Fetecau, J. E. Marsden, K. Mohseni, and M. West [2005], Lagrangian averaging for compressible fluids, *SIAM J. on Multiscale Modeling and Simulation* **3**, 818–837.

Holm, D. and J. E. Marsden [2004], Momentum maps and measure-valued solutions (peakons, filaments and sheets) for the EPDiff equation. In Marsden, J. E. and T. S. Ratiu, edi-

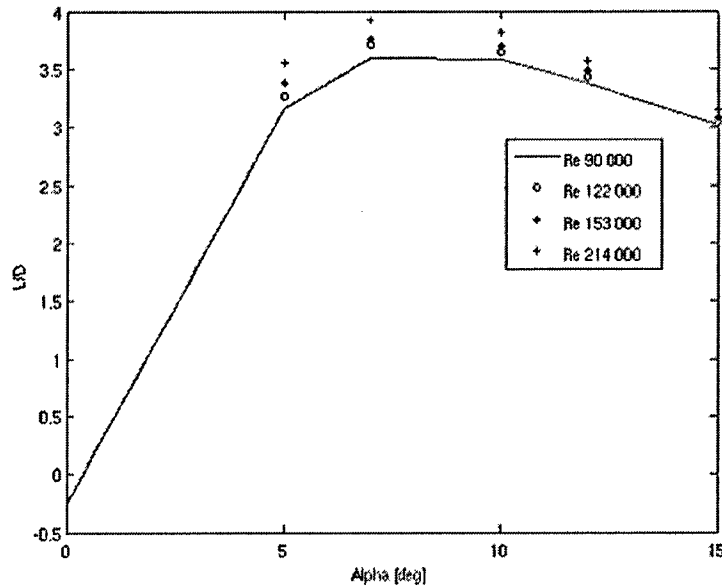


Figure 7.4: C_L/C_D for various Reynolds numbers.

tors, *The Breadth of Symplectic and Poisson Geometry, a Festschrift for Alan Weinstein*, Progress in Mathematics, **232**, pages 203–235. Birkhäuser Boston.

Inanc, T., S. Shadden, and J. E. Marsden [2005], Optimal Trajectory Generation in Ocean Flows, *Proc ACC*, 674–679.

D. Pullin R. Samtaney and B. Kosovic [2001], Direct numerical simulation of decaying compressible turbulence and shocklet statistics. *Physics of Fluids*, **13**, 1415–1430.

K. Mohseni, B. Kosovic, S. Shkoller, and J. Marsden [2003]. Numerical simulations of the Lagrangian averaged Navier-Stokes equations for homogenous isotropic turbulence. *Physics of Fluids*, 15:524, 2003.

H. Zhao, K. Mohseni, and J. Marsden [2004]. Dynamic modeling of α in the isotropic lagrangian averaged navier-stokes- α equations. *2004 ASME International Mechanical Engineering Congress and RD&D Expo*, IMECE2004-61591, 15-21 Nov. 2004, Anaheim, California.

K. Mohseni and H. Zhao [2005]. A priori test of dynamic LANS- α model for turbulent channel flow. *43rd AIAA Aerospace Sciences Meeting and Exhibit*, AIAA2005-0501, 10 - 13 Jan. 2005, Reno, Nevada.

H. Zhao, and K. Mohseni [2004]. A dynamic α model for the lagrangian averaged navier-stokes- α equations. Submitted to *Physics of Fluids*

H. Zhao, K. Mohseni and A. Jameson [2004]. A Helmholtz deconvolution model for incompressible turbulence simulation. In preparation.

K. Mohseni, D. Lawrence, D. Gyllhem, M. Culbreth and P. Geuzaine [2004]. A Flow Simulation around a Micro Air Vehicle in a Plume Characterization Scenario. *3rd AIAA Conference on "Unmanned Unlimited"*, AIAA2004-6598, Sept. 2004, Chicago, IL.

M.R. Waszak and L.N. Jenkins. Stability and control properties of an aeroelastic fixed wing micro aerial vehicle. AIAA paper 2001-4005, August 2001. AIAA Atmospheric Flight Mechanics Conference, Montreal, Canada.